Insights into the behavior of unsaturated diacylglycerols in þÿmixed lipid bilayers in relation to protein kinase molecular dynamics simulation study

Heinonen, Suvi

2022-09-01

Heinonen , S , Lautala , S , Koivuniemi , A & Bunker , A 2022 , ' Insights into the behavior of þÿunsaturated diacylglycerols in mixed lipid bilayers in relation to protein kinase molecular dynamics simulation study ' , Biochimica et Biophysica Acta. Biomembranes , vol. 1864 , no. 9 , 183961 . https://doi.org/10.1016/j.bbamem.2022.183961

http://hdl.handle.net/10138/347472
https://doi.org/10.1016/j.bbamem.2022.183961

BBA - Biomembranes 1864 (2022) 183961

Contents lists available at ScienceDirect

BBA - Biomembranes

journal homepage: www.elsevier.com/locate/bbamem

Insights into the behavior of unsaturated diacylglycerols in mixed lipid bilayers in relation to protein kinase C activation—A molecular dynamics simulation study

Suvi Heinonen[1], Saara Lautala [*,1], Artturi Koivuniemi, Alex Bunker

Drug Research Program, Division of Pharmaceutical Biosciences, University of Helsinki, FI-00014, Helsinki, Finland

ARTICLE INFO

Keywords:
Diacylglycerol
Lipid signaling
Acyl tail unsaturation
Lipid bilayer
Protein kinase C
Molecular dynamics simulation

ABSTRACT

The lipid second messenger diacylglycerol (DAG) is known for its involvement in many types of cellular signaling, especially as an endogenous agonist for protein kinase C (PKC). Evidence has emerged that the degree of saturation of the DAG molecules can affect PKC activation. DAG molecules with different acyl chain saturation have not only been observed to induce varying extents of PKC activation, but also to express selectivity towards different PKC isozymes. Both qualities are important for precise therapeutic activation of PKC; understanding DAG behavior at the molecular level in different environments has much potential in the development of drugs to target PKC. We used molecular dynamics simulations to study the behavior of two different unsaturated DAG species in lipid environments with varying degrees of unsaturation. We focus on phosphatidylethanolamine (PE) instead of phosphatidylcholine (PC) to more accurately model the relevant biomembranes. The effect of cholesterol (CHOL) on these systems was also explored. We found that both high level of unsaturation in the acyl chains of the DAG species and presence of CHOL in the surrounding membrane increase DAG molecule availability at the lipid–water interface. This can partially explain the previously observed differences in PKC activation strength and specificity, the complete mechanism is, however, likely to be more complex. Our simulations coupled with the current understanding of lipids highlight the need for more simulations of biologically accurate lipid environments in order to determine the correct correlations between molecular mechanisms and biological behavior when studying PKC activation.

1. Introduction

Diacylglycerol (DAG) is a lipid second messenger with a structure comprised of a glycerol moiety connected to two acyl chains [1]. This lipid species is associated with several cellular signaling pathways by activating both the classical and novel protein kinase C (cPKC and nPKC) isozymes at the plasma membrane upon extracellular stimulus [2]. The PKC isozyme family consists of serine/threonine kinases, which regulate multiple cellular functions, including cell–cell recognition, proliferation, polarization and migration [3,4]. Abnormalities in PKC signaling have long been linked to the pathophysiology of various diseases such as heart failure, diabetes, Alzheimer's disease and different cancers [5–7]. In Alzheimer's disease, deficient PKC function has been connected to several disease promoting processes [6]. Moreover, clinical data has been obtained that suggests that the loss of function of some PKC isozymes is a possible tumor-promoting mechanism [8]. Considering the pathological relevance of defective PKC function, the discovery and design of DAG-like compounds capable of inducing PKC activation is a very active field of research [4,9].

Despite having a simple structure of a glycerol moiety and two acyl chains, the biophysical characteristics of DAG molecules can vary immensely due to the possible variety in acyl chains. Namely, different DAG molecular species can be classified based on the length and degree of saturation of their acyl chains. In naturally occurring DAG molecules, the *sn*-1 acyl chain is usually saturated or monounsaturated, whereas the *sn*-2 acyl chain is monounsaturated or polyunsaturated [10–12]. Interestingly, this variety comes with differences in ability to activate PKC. Multiple studies have indicated *e.g.* that DAG molecules with two saturated acyl chains are less successful as PKC activators in comparison to unsaturated DAG molecules [13–16]. Some DAG species even seem to have varying levels of activation abilities on specific PKC isozymes, as more recent experiments have shown that different PKC isozymes may have distinct preferences for saturated and unsaturated DAG molecules [17].

* Corresponding author.
E-mail address: saara.lautala@helsinki.fi (S. Lautala).
[1] These authors contributed equally to this work.

https://doi.org/10.1016/j.bbamem.2022.183961
Received 22 December 2021; Received in revised form 2 May 2022; Accepted 4 May 2022
Available online 11 May 2022

Furthermore, differences in the lipid environment surrounding the DAG molecules, such as CHOL content of the membrane, have also been observed to induce differences in PKC activation [18]. The details of the molecular mechanisms behind the different agonist potencies and isozyme-specific effects, however, remain unknown.

So far, DAG effects have mostly been inspected through the lense of allosteric modulation, as the focus has been on the determination of the link between the alterations to the membrane structure, induced by the presence of DAG, and the level of activity [1,19–25]. Studies that attempt to relate PKC modulation to the behavior of DAG molecules themselves by exploring the possibilities of preferential binding, have been relatively scarce, possibly due to the difficulty of probing this behavior experimentally.

Through molecular dynamics (MD) simulations, however, it is possible to develop an understanding of how structural properties relate to the behavior of individual molecules and entire lipid membranes; this has seen broad use in the study of a wide range of phenomena related to biomembranes [26,27]. Recently, we determined that, for the case of non-endogenous PKC agonists, the dynamics and orientation of the agonist molecules at the lipid–water interface do indeed play a substantial role in their binding to PKC [28]. Based on these results, obtaining additional insight into the conformation and location of varying DAG species in different lipid bilayers without the presence of PKC could potentially help explain the acyl-chain dependent effects on DAG induced PKC activation. Even though DAG behavior alone probably will not account for all the variations observed in the activation modes of different PKC isozymes, as protein structure also likely plays a role, inspecting ligand behavior independent of the protein offers an interesting alternative perspective on the matter worth exploring.

Some work has already been conducted in this avenue of research; multiple studies have already applied MD simulation to investigate the behavior of DAG molecules in lipid membranes [21,29,30]. Still, despite the already mentioned vast variety of possible DAG species in existence, only one study by Alwarawrah et al. [23], examined the behavior of multiple DAG molecular species; 1,2-dipalmitoyl-*sn*-glycerol (DPG), 1-palmitoyl-2-oleoyl-*sn*-glycerol (POG) and 1,2-dioleoyl-*sn*-glycerol (DOG). Even in this study, however, the comparison is only made between DAG species with monounsaturated and saturated fatty acids. The behavior of polyunsaturated DAG molecules, experimentally shown to have greater amplification in activity has, as of yet, not been investigated with MD simulations.

Thus, here we compare the behavior of two unsaturated DAG molecules, one di-mono- and one *sn*-2 polyunsaturated, 1,2-dioleoyl-*sn*-glycerol (DOG) and 1-stearoyl-2-docosahexaenoyl-*sn*-glycerol (SDG) (Fig. 1) in our MD simulations. Both of the selected DAG species are biologically relevant, concentrations of both DAG types have been observed to rise following cellular stimulus *in vitro* [10]. Further, they possess differing PKC activation abilities with SDG exhibiting a more potent response than DOG [16]. Intriguingly, SDG has also been observed to be preferred by specific nPKC isozymes [17]. Altogether, these differences make the comparison of these two molecular species particularly interesting.

So far, the majority of both experimental and computational studies of DAG and related lipids have been carried out in phosphatidylcholine (PC) based bilayers [21,22,31,32]. The inner leaflet of the plasma membrane, where DAG induced PKC activation occurs, is, however, enriched with phosphatidylethanolamine (PE) while PC predominantly occupies the outer leaflet [33–35]. In order to gain more accurate insight into the behavior of DAG in its relevant environment we have simulated DAG with two different PE based glycerophospholipids (GPLs), namely 1-palmitoyl-2-oleoyl-*sn*-glycero-3-phosphatidylethanolamine (POPE) and 1-stearoyl-2-docosahexaenoyl-*sn*-glycero-3-phosphatidylethanolamine (SDPE) (Fig. 1). The rationale behind using these two PE species is that PKC function spans across multiple tissue types with differing lipid compositions. The SDPE systems model neural tissue, as the brain is especially enriched with docosahexaenoic acid, whereas POPE was chosen to represent glycerophospholipids with average acyl chain composition in peripheral tissues [26,36,37].

We also examined the role of CHOL on DAG behavior in these bilayers (Fig. 1). As both DAG and CHOL have been known to change the biophysical properties of PC bilayers before [21,23,38], we decided to investigate how these changes relate to the PE-bilayers studied here. Furthermore, simulations with CHOL offer the opportunity to investigate the unknown mechanisms in which CHOL can promote the potency of DAG molecules in activating PKC [18].

The aim of this study is to determine the extent to which acyl chain composition of DAG molecules and the composition of the lipid environment can alter the dynamical features of DAG molecules at the lipid–water interface, and whether these changes offer explanations for the observed specific divergences in PKC activation. In addition, the simulations will further elucidate DAG behavior in a general context and thus also assist in the development of future DAG mimetic molecules.

2. Methods

2.1. The lipid bilayer systems

Eight membrane models were constructed for MD simulations of DAG behavior: DOG/POPE, DOG/SDPE, SDG/POPE, SDG/SDPE, DOG/POPE/CHOL, SDG/POPE/CHOL, SDG/POPE/CHOL and SDG/SDPE/CHOL (see Fig. 2). Additionally, the overall effect of CHOL on the chosen phospholipid bilayers was examined with control systems composed of POPE, SDPE, POPE/CHOL and SDPE/CHOL. Each DAG/GPL system consisted of 12 DAG molecules and 116 GPLs, while the systems with CHOL consisted of 12 DAG molecules, 74 GPLs and 42 CHOL molecules. The control systems consisted either 128 GPLs or 86 GPLs and 42 CHOL molecules. In all systems there were 6400 water molecules, totaling to a lipid hydration number of 50. The initial coordinates for all systems were constructed using the CHARMM-GUI input generator [39–41].

2.2. Force field parameters

All simulations in this study were performed using the Lipid17 forcefield with the TIP3P water model [42–44]. The DAG molecules were parameterized according to the Lipid14 procedure [43], *i.e.* multiconformational RESP fitting [45] was applied for calculating the partial charges of the DAG glycerol moiety, with predefined partial charges from the Lipid11 scheme [46] for the capping groups. The missing bonded parameters of the DOG and SDG *sn*-3-hydroxyl group (OH-group) were set as identical to that of the primary OH-group in phosphatidylglycerol (PG), already present in the Lipid17 force field. Further details regarding the parametrization of the DAG glycerol moiety are found in the Supplementary Material (SM).

2.3. Unbiased molecular dynamics simulations

Molecular dynamics simulations of lengths 2.1 μs (DAG/GPL) and 1 μs (DAG/GPL/CHOL) were performed using the GROMACS-2018.6 simulation package [47–50], while the control simulations were run for 1 μs with GROMACS-2021.2 [51]. The equations of motion were integrated using the leap-frog algorithm with a time step of 2 fs [52]. Electrostatics were controlled using the fast smooth Particle-Mesh Ewald (SPME) with a cut-off distance of 1.0 nm and Fourier spacing of 0.1 nm [53]. The cut-off distance for the Lennard-Jones interactions was 1.0 nm. The length of bonds containing hydrogen atoms were constrained using the LINCS algorithm [54]. All systems were simulated using an isothermal–isobaric ensemble with physiological conditions (310 K temperature and 1 bar pressure). The lipids and water were coupled to separate heat baths using the Nosé–Hoover thermostat [55,56].

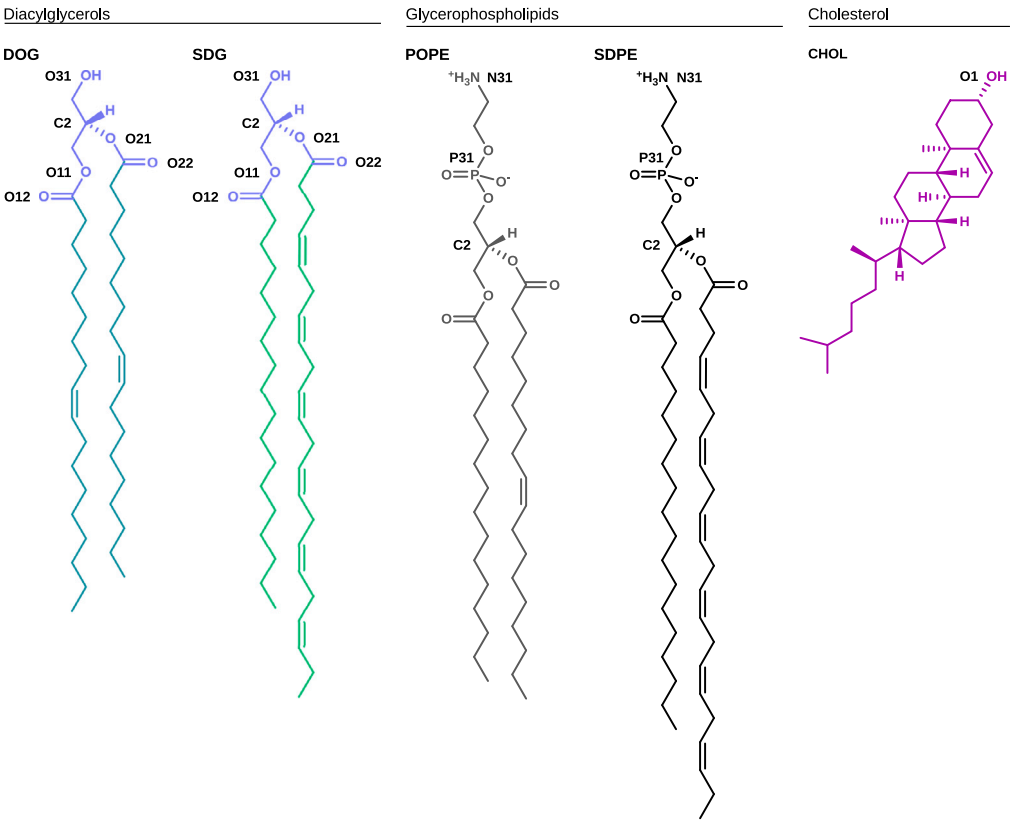

Fig. 1. Chemical structures of 1,2-dioleoyl-*sn*-glycerol (DOG), 1-stearoyl-2-docosahexaenoyl-*sn*-glycerol (SDG), 1-palmitoyl-2-glycero-*sn*-glycero-3-phosphatidylethanolamine (POPE), 1-stearoyl-2-docosahexaenoyl-*sn*-glycero-3-phosphatidylethanolamine (SDPE) and cholesterol (CHOL). The atoms relevant to the analysis are marked separately, and the naming is based on the topology files used in simulations (see Supplementary Material). The glycerol moieties of DOG and SDG in blue.

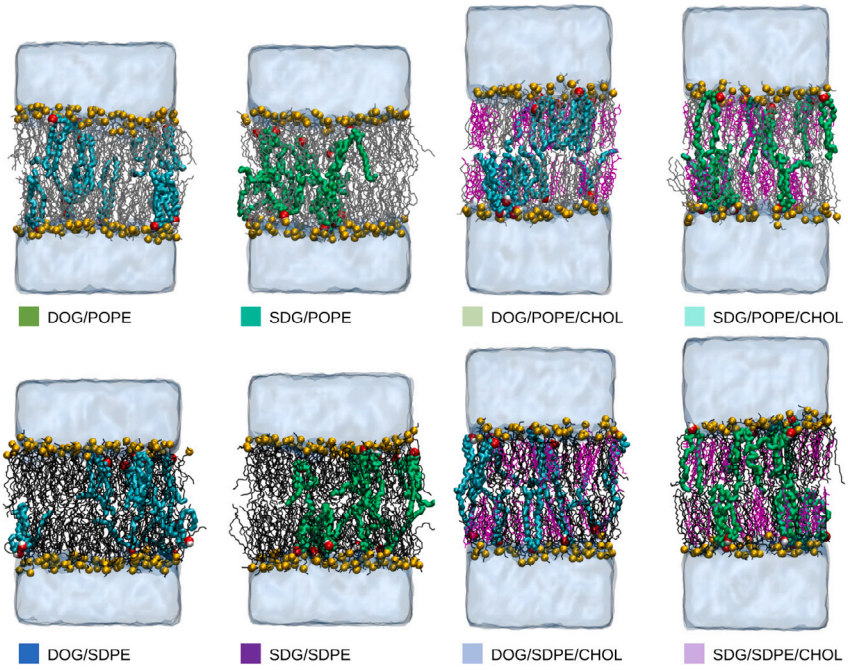

Fig. 2. Snapshots of the eight systems containing DAG at the end of each conventional MD simulation (2.1 μs for DAG/GPL systems and 1 μs for DAG/GPL/CHOL systems). Water molecules are depicted in light blue, the P31 phosphorus atom of the glycerophospholipids in dark yellow, the POPE acyl chains are in black, and the SDPE acyl chains in gray. The DOG molecules are depicted in cyan, the SDG molecules in mint green and CHOL in magenta. In each system, the O31 atoms of DAG molecules are marked with red.

Semi-isotropic pressure coupling was achieved using the Parrinello–Rahman barostat with a compressibility of $4.5e^{-5}$ bar^{-1} with the xy plane and z axis, *i.e.* the membrane normal, coupled separately [57]. The coupling constants for temperature and pressure coupling were 0.4 ps^{-1} and 10.0 ps^{-1}, respectively. All systems reached equilibrium within the first 100 ns of the simulation (see SM, Fig. S1 and Fig. S2), and

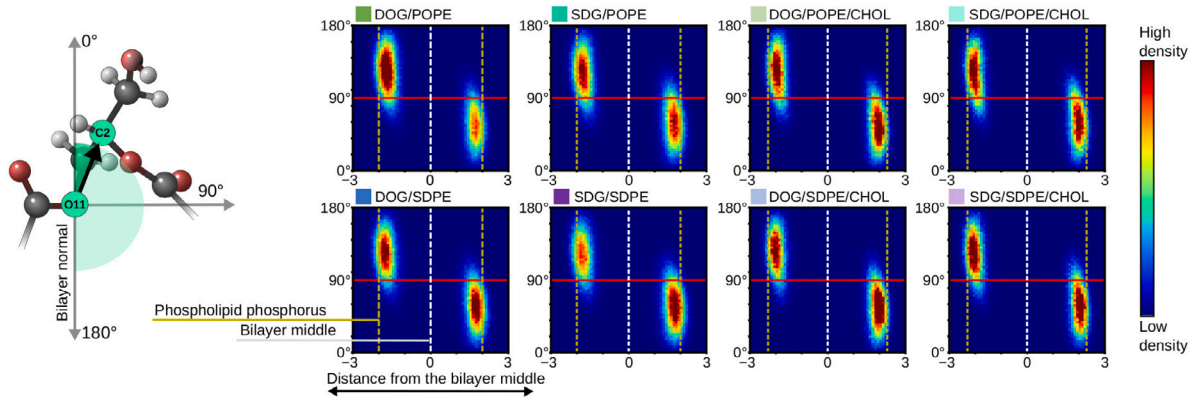

Fig. 3. Analysis of tilt angles of the glycerol moiety of DAG molecules. Left: Illustration of the analysis vector; tilt angles of the presented O11-C2 vector were calculated against the bilayer normal. Right: Heatmaps formed with the calculated tilt angles and the distance of the OH-group from the bilayer center. The yellow dashed line marks the average position of the GPL P31 atoms, white dashed line the bilayer center and red line denotes tilt angle of 90°.

analysis was conducted from that point onward until the end of each trajectory. This meant that for the case of the DAG/GPL simulations the last 2.0 μs and for the DAG/GPL/CHOL and control systems the last 900 ns of the simulations were used for analysis. Further details on the analysis can be found in SM.

2.4. Umbrella sampling

In addition to the analysis of the orientation and dynamics of the systems conducted from the traditional unbiased MD simulations, we also ran force biased MD simulations in order to investigate whether or not the position of the energy minima related to the locations of the different DAG species in the GPL systems differs. This was accomplished by calculating the potential of mean force (PMF) along the membrane normal using an umbrella sampling and weighted histogram analysis method (WHAM) with GROMACS-2018.7 [58]. For simplicity, the four DAG/GPL systems without CHOL were selected for the sampling. In each system, two DAG molecules in each of the bilayer leaflets were selected for analysis to enhance sampling with the same computational cost. To obtain sampling windows, we performed two sets of simulations with the same magnitude of force bias, however in opposite directions along the bilayer normal. In the first set, the DAG molecules were pulled in the direction of the aqueous interface and in the second set towards the bilayer center to capture the full reaction coordinate from the bilayer center to the water phase. The two selected DAG molecules in each leaflet were dragged simultaneously with a force constant of 2000 kJ mol^{-1} nm^{-2} applied to the center of mass (COM) of their OH-group with respect to the corresponding membrane leaflet COM. Altogether 28 sampling windows were extracted from each system at different timepoints. The windows were simulated for 70 ns (80 ns for the SDG/POPE system) using a force constant of 1000 kJ mol^{-1} nm^{-2} and the same simulation parameters as in the previous unbiased MD simulations. Prior to simulating the sampling windows, the exact z-coordinate positions of the four individual DAG molecules in each window were observed to fluctuate slightly in comparison to each other. Thus, effective overlap of the umbrella histograms was ensured by setting the four selected DAG molecules in each simulation window to the same predetermined reference distances 0.1 nm apart extending from 0 to 2.5 nm from the bilayer center to the water phase. The PMF profiles were determined using the gmx wham tool found in GROMACS-2018.7 simulation package [47]. The WHAM analysis was based on the last 30 ns of the simulations and the statistical error estimation was carried out using Bayesian bootstrapping with 100 bootstraps [59,60].

3. Results

Previously DAG molecules have been observed to cause CHOL-like changes to the biophysical properties of lipid bilayers, *i.e.* area per lipid (APL) and membrane thickness [21,23,38]. As most of these studies were conducted for PC systems, we quantified these effects also in our simulated PE systems. In our simulations the effects exerted by DAG molecules on APL and membrane thickness were much smaller. This was somewhat expected, as the condensing effect of CHOL has previously been observed to be less substantial on PE bilayers than on PC bilayers [61]. The results for APL and membrane thickness are presented in Table S1.

To look at the general conformations of the DAG molecules, we calculated the angular distributions of the glycerol moieties. We selected the tilt angle of a vector from the DAG O11 atom to the C2 atom against the bilayer normal as a representation of the overall angle of the glycerol moiety (Fig. 3). The tilt angles are presented here to vary in the range of 0° to 180°. At 90°, the vector is perpendicular to the bilayer normal, whereas 0° represents an upright position towards the first leaflet and 180° towards the opposing leaflet (Fig. 3, left). The tilt angles were plotted against the distances of the COM of the DAG OH-groups from the bilayer center, forming heat maps which are presented in Fig. 3.

The tilt angles of the glycerol moieties of DOG and SDG are very similar to each other regardless of the surrounding GPL environment or the presence of CHOL. The general orientation pattern is preserved across all systems, with the sole difference of a locational shift of population towards the water interface in DAG/GPL/CHOL systems, implying DAG molecules position closer to the lipid–water interface in these systems. The sampling density is highest at approximately within the range of angles of 30 to 80° and OH-group positions of 1.4 to 2.0 nm for DAG/GPL systems, and for DAG/GPL/CHOL systems 30 to 90° and 1.7 to 2.3 nm, respectively. Interestingly, there are a number of occurrences of DAG molecules with the O11-C2 vector turned towards the opposing leaflet in both sets of systems. The population with this vector tilt can be seen in Fig. 3 where the areas of medium sampling density cross the red line. An illustration of such movement is presented in Figure S4.

Next, we investigated the positioning of the DAG molecules in each of the membranes studied. As some thickening was observed in the CHOL enriched systems, we decided to determine the average position of the DAG molecules in the membranes in relation to the surrounding GPL headgroups instead of the absolute distance from the bilayer center. This distance is independent of the membrane thickening, and this way the results concerning the position of the DAG molecules are comparable across all systems. This measurement was accomplished by calculating the distance between the respective C2 atoms of the DAG

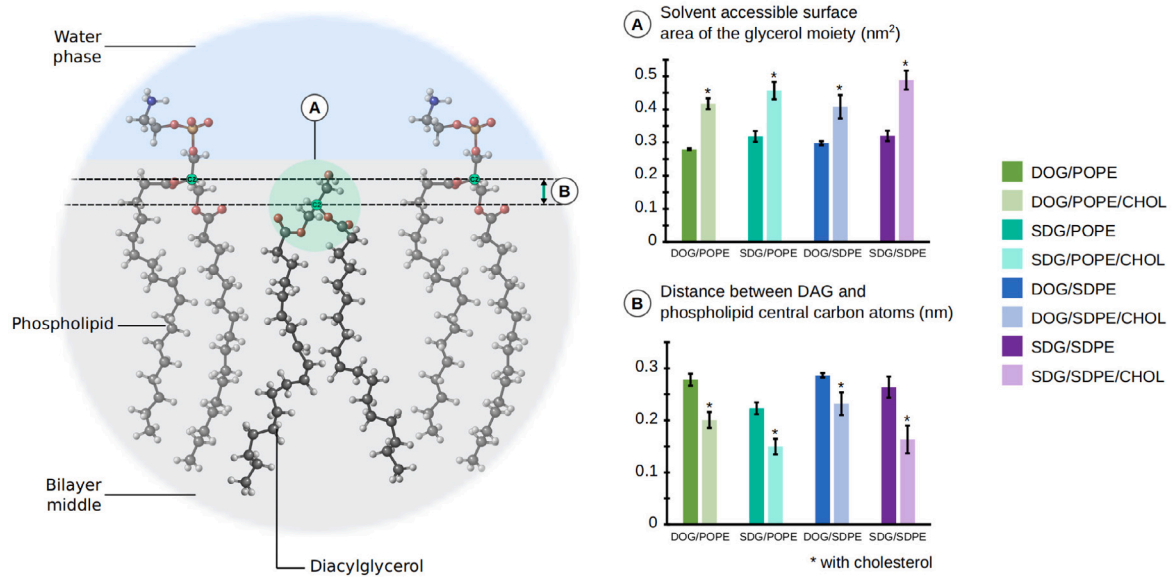

Fig. 4. Graphical representation of DAG species positioning in relation to surrounding the GPLs and degree of exposure to solvent at the lipid–water interface. Graph (A) shows the average solvent accessible surface area of the DAG glycerol moiety, while graph B shows the average distances between C2 atom of DAG molecules and respective C2 atoms of the GPLs.

Table 1
Solvent accessible surface area (nm^2) of different polar groups per DAG molecule. The components presented in the table are the glycerol moiety (GM), hydroxyl group (OH), *sn*-1 ester oxygen (O11), *sn*-1 carbonyl oxygen (O12), *sn*-2 ester oxygen (O21), and *sn*-2 carbonyl oxygen (O22).

	GM	OH	O11	O12	O21	O22
DOG/POPE	0.280 ± 0.003	0.074 ± 0.002	0.0028 ± 0.0002	0.0338 ± 0.0009	0.0019 ± 0.0002	0.0228 ± 0.0008
SDG/POPE	0.32 ± 0.02	0.083 ± 0.005	0.00407 ± 0.00012	0.037 ± 0.002	0.00209 ± 0.00008	0.026 ± 0.003
DOG/SDPE	0.298 ± 0.006	0.078 ± 0.003	0.00270 ± 0.00008	0.0350 ± 0.0009	0.0017 ± 0.0002	0.0250 ± 0.0004
SDG/SDPE	0.32 ± 0.02	0.085 ± 0.004	0.0030 ± 0.0004	0.038 ± 0.002	0.0018 ± 0.0003	0.027 ± 0.002
DOG/POPE/CHOL	0.42 ± 0.02	0.115 ± 0.004	0.0044 ± 0.0004	0.048 ± 0.003	0.0026 ± 0.0005	0.033 ± 0.002
SDG/POPE/CHOL	0.46 ± 0.03	0.124 ± 0.007	0.0054 ± 0.0004	0.051 ± 0.005	0.0028 ± 0.0004	0.036 ± 0.005
DOG/SDPE/CHOL	0.41 ± 0.04	0.110 ± 0.009	0.0034 ± 0.0007	0.047 ± 0.005	0.0018 ± 0.0005	0.033 ± 0.005
SDG/SDPE/CHOL	0.49 ± 0.03	0.133 ± 0.008	0.0055 ± 0.0003	0.055 ± 0.003	0.0026 ± 0.0006	0.039 ± 0.004

molecules and GPLs in the systems. A graphical representation of this distance is illustrated in Fig. 4.

Keeping in line with previous MD simulations [21,23], we observed the equilibrium position of the DAG molecules to be located deeper within the bilayer in comparison to the surrounding glycerophospholipids in all systems (Fig. 4B). In POPE bilayers, the difference between the average distance of the C2 atoms were 0.278 ± 0.012 nm for DOG/POPE and 0.223 ± 0.012 nm for SDG/POPE, respectively. For the case of the SDPE bilayers, the respective differences in average distance were 0.287 ± 0.005 nm for DOG/SDPE and 0.26 ± 0.03 nm for SDG/SDPE. Thus, SDG is on average positioned closer to the GPL headgroup region, while DOG tends to sink deeper within the bilayer. Significant difference, however, was observed only in DAG/POPE bilayers. In DAG/POPE/CHOL systems the distances were 0.201 ± 0.015 nm for DOG/POPE/CHOL and 0.150 ± 0.015 nm for SDG/POPE/CHOL. In the DAG/SDPE/CHOL bilayer these distances were 0.23 ± 0.03 nm for DOG/SDPE/CHOL and 0.16 ± 0.03 nm for SDG/SDPE/CHOL, respectively. The distance between the C2 atoms was notably decreased in all these systems compared to the DAG/GPL systems, and interestingly SDG was significantly closer to the water interface than DOG in both the POPE and SDPE systems. Furthermore, the decreases in C2 atom distances in DAG/POPE/CHOL systems compared to the DAG/POPE systems were similar for both DAG species; 28 ± 7% (0.08 ± 0.02 nm) for DOG/POPE/CHOL, and 33 ± 8% (0.07 ± 0.02 nm) for SDG/POPE/CHOL, while in the DAG/SDPE/CHOL systems the same decrease was somewhat different between the two DAG species. In the DOG/SDPE/CHOL the decrease compared to DOG/SDPE was 19±8% (0.05±0.03 nm), while the same decrease was 38 ± 12% (0.10 ± 0.04 nm) for SDG/SDPE/CHOL.

These results, however, do not fully describe the extent to which the molecules are exposed to the solvent. Thus, we calculated the solvent accessible surface area (SASA) for the entire glycerol moieties (GM), OH-groups, O11, O12, O21 and O22 oxygen atoms, for the DAG molecules in both sets of systems (see Fig. 4A and Table 1). In general the SASA values of GM of SDG are larger than those of DOG. Within all systems, the order of magnitude of the SASA values across the subgroups is the same; OH has the largest value, followed by the oxygen atoms in the order of O12 > O22 > O11 > O21. These trends are the same in both DAG/GPL and DAG/GPL/CHOL systems, however in DAG/GPL/CHOL systems the SASA values are, overall, larger.

Another useful measure of exposure to polar solvent is the number of hydrogen bonds formed between solvent and solute. Based on the SASA values, we calculated the hydrogen bonding between water and the OH-groups or carbonyl oxygens of the DAG molecules. The results are presented in the left half of Table 2.

In all DAG/GPL systems, each DAG OH-group forms approximately one hydrogen bond with solvent water, whereas hydrogen bonding between water and the carbonyl oxygens occurs to a significantly lower extent. Out of the two carbonyl oxygens, O12 appears to be more available for hydrogen bonding with water than O22, matching the SASA results. Compelling differences between DOG and SDG inside either DAG/GPL or DAG/GPL/CHOL systems are not present. In general, however, slightly more hydrogen bonding was observed to occur in the DAG/GPL/CHOL than in DAG/GPL systems, again matching with the SASA results.

While hydrogen bonding with water is an indicator of exposure, hydrogen bonding with the surrounding membrane lipids can also be used here to study how strongly the DAG molecules interact with the

Table 2
Number of hydrogen bonding in the DAG molecule hydroxyl groups (OH), *sn*-1 carbonyl oxygens (O12) and *sn*-2 carbonyl oxygen (O22) with water and lipid environment (GPL or GPL/CHOL) in different systems. The results are average values presented with error.

	Water			Membrane (GPL or GPL/CHOL)		
	OH	O12	O22	OH	O12	O22
DOG/POPE	0.969 ± 0.008	0.590 ± 0.009	0.446 ± 0.007	0.374 ± 0.014	0.0150 ± 0.0012	0.014 ± 0.003
SDG/POPE	1.01 ± 0.03	0.61 ± 0.02	0.465 ± 0.014	0.379 ± 0.008	0.0165 ± 0.0009	0.0146 ± 0.0005
DOG/SDPE	0.963 ± 0.013	0.635 ± 0.008	0.471 ± 0.002	0.355 ± 0.013	0.014 ± 0.002	0.013 ± 0.002
SDG/SDPE	0.99 ± 0.03	0.63 ± 0.02	0.472 ± 0.014	0.36 ± 0.01	0.0011 ± 0.0009	0.0137 ± 0.0012
DOG/POPE/CHOL	1.112 ± 0.013	0.67 ± 0.03	0.514 ± 0.008	0.330 ± 0.006	0.020 ± 0.003	0.021 ± 0.003
SDG/POPE/CHOL	1.13 ± 0.03	0.680 ± 0.015	0.53 ± 0.03	0.336 ± 0.014	0.0244 ± 0.0013	0.026 ± 0.005
DOG/SDPE/CHOL	1.08 ± 0.05	0.69 ± 0.04	0.54 ± 0.03	0.326 ± 0.015	0.019 ± 0.003	0.023 ± 0.003
SDG/SDPE/CHOL	1.16 ± 0.03	0.73 ± 0.02	0.56 ± 0.02	0.320 ± 0.012	0.026 ± 0.004	0.028 ± 0.008

membrane environment; these interactions are presented in the right column of Table 2. In general hydrogen bonding between DAG and the membrane occurs much less frequently than with water. Essentially only the OH-group forms hydrogen bonds with the membrane, while the bonding mediated by the DAG O12 and O22 is negligible. As is the case with water, there is no difference observed concerning the extent of hydrogen bonding between the two different DAG species and the rest of the lipid membrane.

In addition to forming hydrogen bonds with the environment, the significantly smaller OH-headgroups of the DAG molecules have been observed to affect the GPL headgroup conformations, for example increasing the space between the GPL headgroups [1]. In a previous study Alwarawrah et al. [21] showed that in POPC bilayers the PC headgroups clearly tilt towards DAG and CHOL molecules. As this interaction minimizes the unfavorable interactions by shielding the hydrophobic region of the DAG or CHOL molecules from the solution, it has been named the umbrella effect [21,62].

As their study was conducted in POPC, we wanted to see whether or not the effect translates also to POPE. We thus calculated the 2D radial distribution functions (RDFs) for POPE N31 and P31 atoms around DAG O31 and CHOL O1 atoms to determine the umbrella coverage. These results are presented in Fig. 5. Only the RDF curves for CHOL showed clear peaks indicating it receives umbrella coverage from the GPLs. No distinct peaks, and subsequently no substantial coverage is present for the DAG molecules. As Alwarawrah et al. [21] conducted their simulations with a different lipid species and concentrations from ours, we decided also to repeat some of the POPC simulations for a more equitable comparison of behavior. The description and results of these simulations can be found in Fig. S3. These results were in agreement with those obtained for the systems with PE-GPLs, as the absensence of umbrella coverage for DAG molecules is evident from them as well.

We also calculated the PMF along the membrane normal for the DAG molecules, as we were interested to investigate their transverse motion and tendency to position in different regions of the membrane in the DAG/GPL systems (Fig. 6). When all four PMF profiles are plotted together (6, left), it becomes evident that between the two DAG species the energetics of transbilayer movement are similar. As the DAG molecules are moved from the center of the bilayer towards the water phase, the PMF first exhibits a slight increase, before falling into the energy minimum slightly below the position of the phospholipid P31 atoms. Following the well a steep ascend begins until end of analysis in the aqueous phase.

In fact, the PMF curves seem to be mainly governed by the surrounding GPL rather than the specific DAG molecular species (6 center and right). A visible gap is created between the curves related to POPE and SDPE systems in the range of distances 0.5–1.5 nm from the bilayer center. Towards the minima of the energy wells this gap becomes less notable.

As the simulations with only DAG/GPL failed to show compelling differences, we deemed repeating the umbrella sampling simulations for the DAG/GPL/CHOL systems too large of a computational effort compared to the probability of obtaining meaningful insight. Furthermore, it is well known that in systems more complex than two components, the lateral asymmetry around the pulled molecules could cause problems in sampling the entirety of the phase space.

4. Discussion

Understanding DAG behavior is crucial for achieving efficient PKC targeting and selective therapeutic activation. Numerous studies have already considered the role of DAG as a modulator of PKC through its alteration of the physical characteristics of the lipid bilayers it inhabits [1,20], but studies focusing on the effect that DAG acyl chains have on the direct regulation of the initial translocation and preferential membrane binding of PKC have so far been relatively scarce. Furthermore, the research that has been conducted in this prospect has so far evaded the biologically relevant PE bilayers, as it has so far largely focused on saturated species in PC bilayers. This has left many possible aspects of DAG PKC modulation relatively unexplored. To broaden the current understanding, we have in this research investigated the behavior of two unsaturated DAG molecules, DOG and SDG, in four different PE-membrane environments. The membrane environments were either monounsaturated POPE or polyunsaturated SDPE, with and without CHOL included in the mix. Our intention was to observe how the differences in acyl chain length and saturation degree as well as changes in the surrounding membrane environment affect the behavior of these DAG molecules. As we are interested in DAG molecules in the context of PKC activation, it was clear since the beginning that studying the availability of DAG molecules at the lipid–water interface of the membrane through position, orientation and conformations would be crucial.

The SASA and C2–C2 distance calculations showed a trend of SDG molecules both being more exposed to solvent and positioning closer to the aqueous interface of the lipid bilayer than DOG within POPE bilayers. In SDPE bilayers, the difference was not as significant, but a similar trend could be observed. Inclusion of CHOL into the bilayers brought both DOG and SDG closer to the surface of the bilayer, but the effect was strongest for SDG in SDPE in both the C2–C2 distance and SASA calculations. Previous computational work has already suggested that unsaturated DAG species would position closer to the lipid–water interface in membranes in comparison to saturated species [23]. Our results on DOG and SDG seem to confirm that similar differences in membrane position occur also between di-mono and *sn*-2 polyunsaturated DAG molecules. Thus they offer support to the original observations made by others and further show that the more unsaturated the DAG species is, the higher it will likely sit in the lipid bilayer. This higher positioning and exposure of unsaturated DAG molecules could serve as an explanation for the experimental observations of increased PKC activation related to them [13–16]. It can be argued that the increased exposure of the unsaturated DAG species make the molecules more readily available for binding with the protein and that increases their potency on PKC. The structure of the C1b domain of PKCδ supports

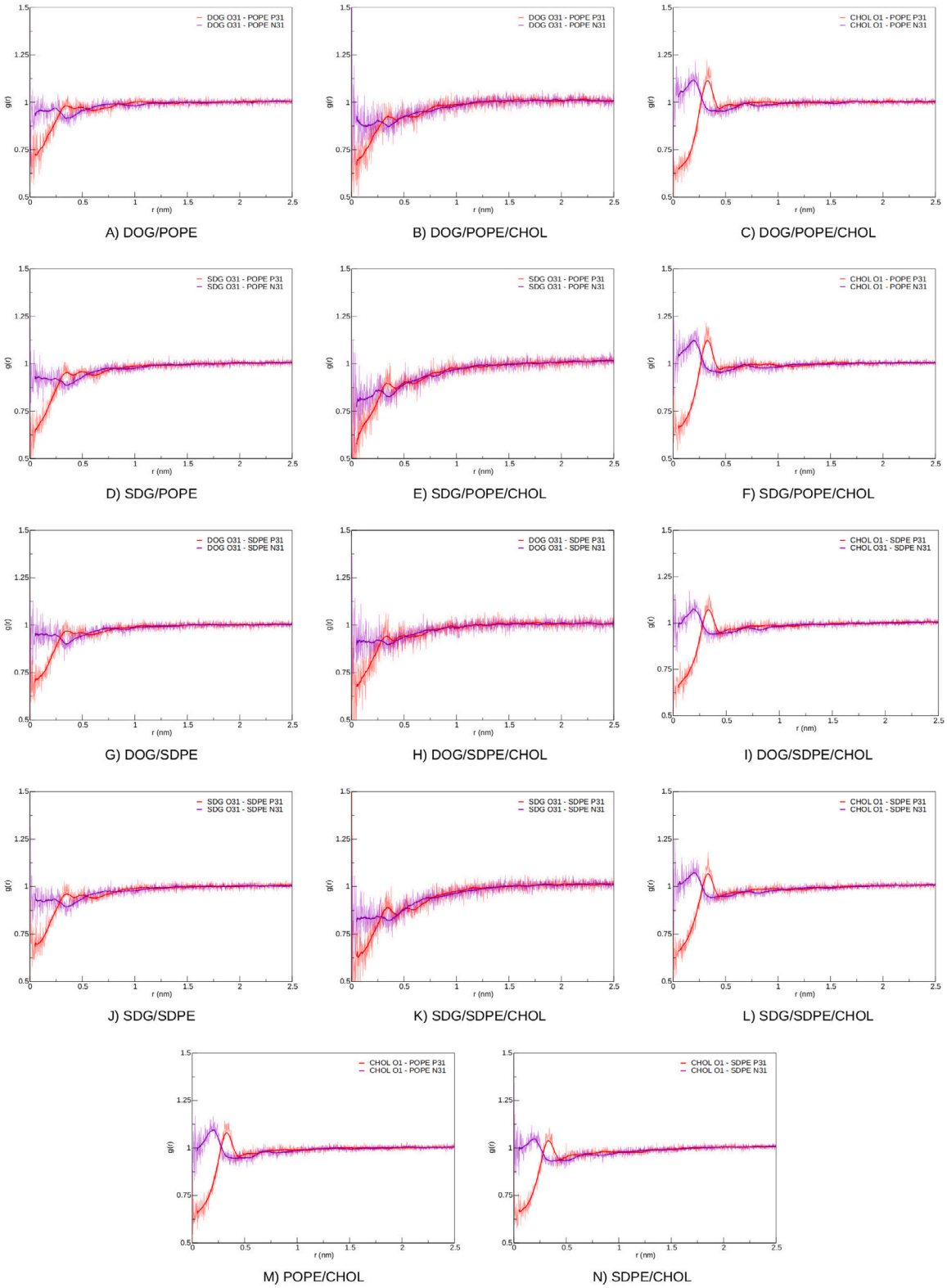

Fig. 5. Radial distribution functions (RDF) illustrating the umbrella coverage of both DAG and CHOL by the PE headgroups in each system. The function $g(r)$ is evaluated in the xy-plane parallel to the bilayer, while the distance r is the spatial distance between the reference atom and the selected atom in this plane. Figures A–L show the RDF between DAG O1 and GPL P31/N31 first in DAG/GPL systems, then the same for DAG/GPL/CHOL systems, and finally the RDF between the CHOL O1 and GPL P31/N31 for each system. Figures M and N shows CHOL O1- GPL P31/N31 RDFs for the control systems.

this, as when unligated the binding site is occupied with water creating hydrogen bond bridges inside of the cleft [63]. Thus, insertion of this structure deep into the bilayer would either require dehydration of the cleft, or insertion of water into the lipid bilayer, both of which are energetically unfavorable situations [63,64]. If the DAG molecule is readily available on the membrane surface and subsequently well

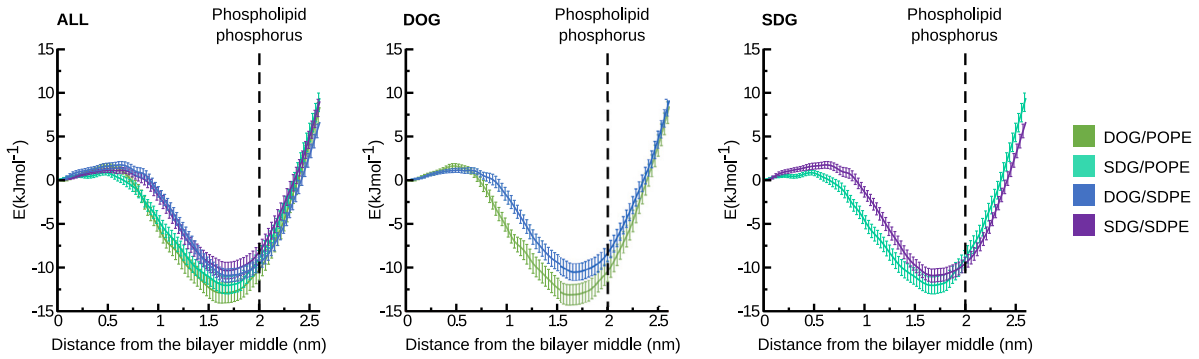

Fig. 6. Potential of mean force (PMF) on the DAG OH-group as the function of its position along the bilayer normal. Position 0 nm represent the bilayer center, and 2.5 nm the beginning of the water phase. On the left, the PMF profiles from all four DAG/GPL systems, and then the PMF profiles for DOG and SDG systems individually, respectively. The dashed line marks the average position of glycerophospholipid P31 atoms.

hydrated, neither of these mechanisms need to happen in order for the binding to occur. Thus, the increased hydration of DAG headgroups as presented by the increased SASA values, could actually lead to more favorable energetics in binding. Exactly stating this based on our simulations is not possible, but these energetics could be explored with conducting thermodynamic integration simulations with the protein present as PKC binds to DAG molecules both highly exposed and more deeply buried in the membrane.

We are confident the qualitative trend we observed here for the highly unsaturated SDG positioning higher than DOG in the membrane is clear enough to be considered as a reason for the increased activity caused by polyunsaturated DAG molecules observed previously in experiments. The fact that the addition of CHOL into the systems shortened the C2–C2 distances and increased SASAs all across the systems provides another hint in this direction, as presence of CHOL has been observed to increase the activation of PKC [18].

The increased activation ability, however, is not the sole attribute related to the unsaturation of DAG molecules. In fact, there is evidence of novel PKC isozymes (nPKC) having more of a preference towards unsaturated DAG species than classical PKC isozymes (cPKC) [17]. This preference could relate to the slightly different mechanism of activation between the two isozyme families [2]. In PKCs the domains responsible for membrane recruitment and the beginning of activation are the C1 and C2 domain. The C2 domain binds anionic lipids, while the C1 binds mainly DAG, even though it is also capable of binding phosphatidylserine (PS) [2,65,66]. All nPKC isozymes rely heavily, some solely, on C1 domain interactions with the membrane for their translocation to the cytosolic leaflet of the plasma membrane. Thus to compensate for only having one domain interacting with the membrane the C1 domain in some nPKC isozymes binds DAG with double the affinity than the C1 domains in cPKCs [65,66].

Meanwhile, classical isozymes utilize the C2-domain for this first [2]. Theoretically, the attractive interactions between the C2 domain and the membrane could allow the classical PKCs to diffuse along the membrane plane after the initial C2 recruitment, while nPKCs need to engage the DAG molecules as the very first interaction. This could mean the cPKCs might have better prerequisites to seek the more deeply buried saturated DAG after initial contact, as the C2 domain already directs the protein to the vicinity of the DAG molecules. It could thus be argued, that the preference towards unsaturated DAG molecules in nPKCs stems at least partly from the higher positioning of the DAG molecules; this way forming the main recruiting interaction is more probable, as the DAG is more readily available at the cytosolic membrane interface. Meanwhile, cPKCs can find DAG molecules both at first contact and while diffusing along the plane, and it explains why they do not show such a specific preference towards the more unsaturated species. Thus our results of higher positioning of the unsaturated DAG species could be seen to support both the activity increase and isozyme specificity. It is important, however, to keep in mind that the mechanism of action is probably not this straightforward, as different highly unsaturated DAG species also have been observed to activate both cPKC and nPKC isozymes differently [67]. Protein structure does likely have a considerable effect as well, and the resulting mechanism is a complex interplay between DAG behavior, membrane effects and protein structure.

Based on these results we expected the unsaturated DAG molecules to also form more hydrogen bonds at the interface. Interestingly, in our analysis there was no notable difference between DOG and SDG in number of hydrogen bonds. However, the hydrogen bonding of the DAG molecules is not only interesting in terms of exposure, but also in an effort to see whether the specific hydrogen bonding patterns would differ between the two species, possibly offering further explanation for the observed the isozyme specificity.

Previously Ryckbosch et al. [68] demonstrated that specific hydrogen bonding patterns in PKC-targeting ligands at the lipid–water interface are linked to the existence of two differing states of the ligand–protein complex in the membrane. In their simulations, the potentially therapeutic bryostatin 1, which formed the stabilizing coordinated hydrogen bonds with water, was observed to occupy two distinct states, one shallow and one deep, while the tumor promoting phorbol ester PDBu and a modified bryolog, lacking the water-coordinating functional groups, only resided in the deep state. Based on this observation, they propose that the therapeutic potential of bryostatin 1 could be solely caused by the existence of this shallow state enabled by the specific hydrogen bonding pattern.

Thus, there could have been some similar differences in the hydrogen bonding between the two DAG species studied here, however, we observed little difference. Granted, the glycerol moiety is preserved between the two species unlike the case for bryostatin 1 and PDBu thus the lack of difference is expected. Two aspects in theory could have created differences in the hydrogen bonding patterns between the two species; (1) the change in depth between DOG and SDG and (2) the positional re-arrangement of the polar subgroups in the glycerol moiety due to varying acyl chains. The change in depth, however, stays within the hydrated region of the bilayers, thus the microenvironment around the GM stays the same regardless. Also, based on our simulations, neither the general arrangement of the subgroups (data not shown) nor the tilt angles were changed between the species, so no change in hydrogen bonding pattern is reasonable from this point of view as well.

Altogether the general pattern of conformations in DAG GMs seems to be quite preserved, although our results indicate a wide distribution of the GM tilt angles across all systems even in systems with CHOL enrichment. This indicates that both DAG species have high flexibility and mobility of the interacting moiety. In fact, high flexibility has been observed to be beneficial in non-native ligands; Yang et al. [69] discovered that the phorbol ester PDAc, a tumor promoter, is more rigid than the potentially therapeutic bryostatin. This could suggest that mimicking the flexibility of DAG GM could be one option in future

designs of PKC targeting ligands. Combined with the observations of bryostatin 1 possessing multiple favorable states in the membrane, could point to the fact that successful activation of PKC by DAG transcends the binding of DAG, and could relate to availability of protein–protein interactions needed for the subsequent steps of signal transconduction, as Ryckbosch et al. suggest [68]. As a whole, our simulations of DOG and SDG showed quite minor differences between the two species. Regarding applicability, however, our results can help guide the design of DAG analogues for therapeutic purposes in the future.

It is important to remember that in the case of PKC, the larger context of membrane interactions must not be disregarded. Recently, MD simulations of PKC targeting ligands revealed membrane related interactions as the defining factor behind the failure of some candidates [28]. For this reason, we wanted to look at the DAG behavior as a function of the surrounding membranes as well.

Our PMF calculations in fact suggest that the transbilayer movement of DAG molecules is more hindered in POPE bilayers compared to the more unsaturated SDPE and that DOG behavior might be, to a small extend, dependent on the extent of unsaturation in the surrounding GPLs. While the desorption of both DOG and SDG is unaffected by change in the surrounding GPL unsaturation, out of all profiles the energy well is deepest for the DOG/POPE system and the shallowest for the DOG/SDPE system. The first observation could be explained by DOG/POPE being the most rigid combination of all and the second observation with steric hindrance; even though the SDG/SDPE mixture is the most fluid, the length of SDG *sn-2* acyl chain might start to hinder the transbilayer movement.

Furthermore, membrane interactions have already been suggested to affect the PKC activation properties of DAG molecules. The umbrella effect has been proposed by Alwarawrah et al. [21] as a reason for the CHOL induced increases in DAG related PKC activation, possibly through competition for the limited umbrella coverage. Our RDF results show evidence of similar interactions, but in significantly smaller magnitudes. Interestingly, the shape of the RDF curves previously presented for POPC actually correspond better to those of POPE in our simulations. Nonetheless, as a whole we were unable to detect the umbrella coverage of DAG molecules in the previously reported magnitudes, even with matching concentrations of components. The reasons for the observed differences in the two set of simulations could stem from the different choice of force fields. Alwarawrah et al. [21] used Berger lipids together with the GROMOS united-atom force field, while we made use of the more modern Lipid17 at our disposal. In the ten years that have passed since the publication of this paper, the original Berger lipids force field has been shown to have too strong attractive force cross-terms in some cases [70]; it is possible this could contribute into the magnitudes of the previous RDF results discussed here. The competitive setting between DAG and CHOL molecules, however, is supported to an extent by our simulation. A slight dip in the number of POPE P31 and N31 atoms around the DAG O31 once CHOL is added in Fig. 5. Recent studies using CHARMM36 forcefield support our findings, as they also found only a weak preference for the neighboring lipid headgroups to locate over cholesterol [71–73]. These studies suggest, that the addition of cholesterol allows for a more free rotation of the lipid headgroups, possibly due to the increased spatial distance between them that cholesterol permits.

Thus, based on these results combined with our findings on RDF and the aforementioned SASA, we propose that when CHOL is present relative to the concentration of DAG in the correct ratio, the extent of umbrella coverage that is available for DAG is even further decreased. The increased space around the DAG headgroups could well increase the availability of DAG headgroups to PKC, and thus explaining why the addition of CHOL increases PKC activity in POPC bilayers that is observed experimentally [13–16,18].

Force fields aside, we would like to further discuss, if it is actually worth questioning using PC lipids as the main lipid component in PKC related simulations. The inner plasma leaflet has PE as the dominant lipid species, and naturally the interactions in the lipid headgroup region are different for this lipid than they are for the case of PC. This leads to the question of whether the PC models actually are describing what happens in the biological systems; some results can be directly extrapolated from PC to other lipids, but especially in current times when simulation resources are not as scarce, one should consider at least running PE simulations together with PC simulations when dealing with the inner leaflet of the plasma membrane.

Evidence exists that PE directly can affect PKC function, such as the observation of PKC behaving abnormally in cells that have purposefully been depleted of PE, and the missing PE has been replaced with PC [74]. In fact evidence of PE being able to compensate for PS in the activation process has also emerged, as membranes containing PE and DAG only were able to induce PKC activity, while PC/DAG membranes could not [75]. It has also been observed that changing the membrane composition from pure PS to 50/50 PS/PE increases PKC activity, while the same substitution with PC lowers the activity [76].

A possible explanation comes from the differences in the respective headgroups. The smaller headgroup of PE would seem to offer a better interaction with PKC than the larger PC [75]. However, the correlation likely is not exactly straightforward, as PE has been observed to also cause inhibitory effects in certain conditions, particularly when presented in excess [77]. It has thus been proposed that the change in activity could stem from the geometric changes the headgroup size difference imposes on the lipids. While PE is a conical lipid that prefers negative curvature, PC is of cylindrical shape and forms flat membranes [37]. Thus PE has a greater propensity to form non-bilayer phases, such as the inverted hexagonal (H_{II}) and cubic phase in comparison to the case for PC [76,77]. This discrepancy in propensities for membrane defects and non-lamellar phases can also explain why with PE membranes the acid tail composition seems to effect the activation patterns much more than with PC [76]. In PC, acyl chain composition has little effect on this propensity, but in PE the propensity for non-lamellar phases increases with acyl chain unsaturation; POPE forms lamellar phases (L_a) at physiological temperatures, SDPE is known to exist in nonlamellar H_{II} phase even in the physiological temperature of 37 °C [78]. The effect of cholesterol on the formation of nonlamellar phases is concentration dependent; at low mol% cholesterol tends to promote nonlamellar phase transitions but in high concentrations the effect is the opposite [79,80]. In addition, CHOL is also known to cause defects in the lamellar phase, and this effect has previously been tied to the increase in activation [18].

Besides PE, DAG itself also has the potential to have perturbing effects on membranes [22,77]. As conical lipids with a small headgroup-to-tail ratio, DAG molecules also impose intrinsic negative curvature strain on the lipid membrane, leading to reduced the transition temperature from lamellar to nonlamellar phases. Studies with PE membranes have shown phase transition to H_{II} to occur even as low as 1 mol% of DAG [81]. In the context of biological systems, however, lipids tend to be arranged as lamellar bilayers [19,82]. Some cell membranes do express quite extreme curvature, such as mitochondrial membranes, Golgi apparatus and endoplasmic reticulum, but plasma membranes, especially in the absence of proteins, are less likely to express such extreme curvature [19,83]. The lipids with non-lamellar tendencies likely mainly affect the overall physical properties of this bilayer, rather than introducing localized domains of non-lamellar phases. Such properties include the intrinsic curvature of the membrane, lateral pressure and packing of the lipids in the structure [19,82].

The presence of negative curvature introducing lipids has been correlated with increased PKC activity, however, it seems that the intrinsic curvature and the correspondent strain do not directly modulate the activation of PKC [84], as PKC activation happens also in Triton micelles with intrinsic positive curvature [85], the intrinsic curvature of PE lipids has no effect of PKC activation [86], and the formation of cubic phases, which in fact reduces curvature strain, has been

observed to increase PKC activation [87]. Thus it is more likely, that modulation is due to some other physical effects, which are nonetheless correlated with the intrinsic curvature and the propensity of forming of non-lamellar phases of the lipid species [19,76].

One much discussed feature linked to DAG-induced curvature stress is the physical shape of the membrane. The physical shape has been proposed to affect both membrane energetics as well as offering the optimal orientations for lipid ligands through allosteric modulation [88]. Separating between cause and effect in the case of curvature, stress and shape however is not unambiguous, as properties of the lipids comprising the membrane and the proteins interacting with it can both induce changes in membrane morphology [88].

These correlations, and subsequent PKC activation patterns, such as isozyme specificity through all-atom MD simulation are however beyond the reach of our current model and present a fully independent area of research. While our model was designed to focus on DAG exposure to PKC, excluding the membrane shape as an allosteric regulator, such models could quite easily be constructed using significantly larger amounts of lipids. Furthermore, inclusion of the protein structure to future simulations, at least the PKC C1 domain, will be crucial for comprehensive understanding.

Considering these findings together with our own, it could be possible that the membrane strain and curvature could well contribute in the manner we observed in our simulations, *i.e.* by DAG molecules being pushed towards the water interface as the membrane curvature and defects increase the tensions in the bilayer.

5. Conclusions

We used both conventional molecular dynamics simulation and umbrella sampling to study how acyl chain unsaturation in DAG molecular species affects the position and dynamics of these molecules in a set of relevant hydrated bilayers in relation to PKC activation.

Our simulations found that both increasing the extent of unsaturation in the DAG molecule acyl chains and the addition of CHOL to the membrane composition increase the degree of exposure to solvent of the DAG molecules. This offers a possible explanation for the observed increase in PKC activity associated with both, in particular, in the context of the mechanism found by Ryckbosch et al. [68]. This difference in positioning in the membrane and exposure could possibly also to be an important factor in more isozyme specific PKC activation.

Overall, however, our results are not quite conclusive enough to fully explain why the two DAG molecular species have been observed to have different levels of PKC activation; we argue that our results are part of a bigger picture.

We propose that more simulations and experiments in biologically relevant environments are needed to shed light on the behavior of these simple molecules in a complex environment, and their implications for the activation of this wildly perplexing enzyme, PKC.

Declaration of competing interest

The authors declare that they have no known competing financial interests or personal relationships that could have appeared to influence the work reported in this paper.

Data availability

Atomic Coordinates and Topologies have been shared as Supplementary Material, other data available upon request.

Acknowledgments

The authors thank the University of Helsinki Doctoral Programme of Drug Research for financing this research. All simulations were carried out using the resources provided by CSC IT Center for Science Ltd.

Appendix A. Supplementary data

Supplementary material related to this article can be found online at https://doi.org/10.1016/j.bbamem.2022.183961.

- Details of parametrization of DAG molecules, equilibration and analysis. Additional data describing areas per lipid, membrane thickness, umbrella coverage in POPC bilayers and lipid flipflop.
- Atomic coordinates for all systems simulated in this research and topology files for DOG, SDG, POPE, SDPE, POPC and CHOL molecules.

References

[1] F.M. Goñi, A. Alonso, Structure and functional properties of diacylglycerols in membranes, Prog. Lipid Res. 38 (1) (1999) 1–48.
[2] A.C. Newton, Protein kinase C: perfectly balanced, Crit. Rev. Biochem. Mol. Biol. 53 (2) (2018) 208–230.
[3] C. Rosse, M. Linch, S. Kermorgant, A.J.M. Cameron, K. Boeckeler, P.J. Parker, PKC and the control of localized signal dynamics, Nat. Rev. Mol. Cell Biol. 11 (2) (2010) 103–112.
[4] A.X. Wu-Zhang, A.C. Newton, Protein kinase C pharmacology: Refining the toolbox, Biochem. J. 452 (2) (2013) 195–209.
[5] V. Talman, A. Pascale, M. Jäntti, M. Amadio, R.K. Tuominen, Protein kinase C activation as a potential therapeutic strategy in alzheimer's disease: Is there a role for embryonic lethal abnormal vision-like proteins? Basic Clin. Pharmacol. Toxicol. 119 (2) (2016) 149–160.
[6] D.L. Alkon, M.-K. Sun, T.J. Nelson, PKC signaling deficits: a mechanistic hypothesis for the origins of Alzheimer's disease, Trends Pharmacol. Sci. 28 (2) (2007) 51–60.
[7] E.M. Griner, M.G. Kazanietz, Protein kinase C and other diacylglycerol effectors in cancer, Nat. Rev. Cancer 7 (4) (2007) 281–294.
[8] A.C. Newton, J. Brognard, Reversing the paradigm: Protein kinase C as a tumor suppressor, Trends Pharmacol. Sci. 38 (5) (2017) 438–447.
[9] M. Rui, R. Nasti, E. Bignardi, S.D. Volpe, G. Rossino, D. Rossi, S. Collina, PKC in regenerative therapy: New insights for old targets, Pharmaceuticals 10 (2) (2017).
[10] M.S. Pessin, D.M. Raben, Molecular species analysis of 1,2-diglycerides stimulated by a-thrombin in cultured fibroblasts, J. Biol. Chem. 264 (15) (1989) 8729–8738.
[11] T.R. Pettitt, M. Zaqqa, M.J.O. Wakelam, Epidermal growth factor stimulates distinct diradylglycerol species generation in Swiss 3T3 fibroblasts: Evidence for a potential phosphatidylcholine-specific phospholipase C-catalysed pathway, Biochem. J. 298 (3) (1994) 655–660.
[12] T.R. Pettitt, A. Martin, T. Horton, C. Liossis, J.M. Lord, M.J.O. Wakelam, Diacylglycerol and phosphatidate generated by phospholipases C and D, respectively, have distinct fatty acid compositions and functions: Phospholipase D-derived diacylglycerol does not activate protein kinase C in porcine aortic endothelial cells, J. Biol. Chem. 272 (28) (1997) 17354–17359.
[13] A. Kishimoto, Y. Takai, T. Mori, U. Kikkawa, Y. Nishizuka, Activation of calcium and phospholipid-dependent protein kinase by diacylglycerol, its possible relation to phosphatidylinositol turnover, J. Biol. Chem. 255 (6) (1980) 2273–2276.
[14] T. Mori, Y. Takai, B. Yu, J. Takahashi, Y. Nishizuka, T. Fujikura, Specificity of the fatty acyl moieties of diacylglycerol for the activation of calcium-activated, phospholipid-dependent protein kinase, J. Biochem. 91 (2) (1982) 427–432.
[15] G. Masayoshi, K. Sekiguchi, H. Nomura, U. Kikkawa, Y. Nishizuka, Further studies on the specificity of diacylglycerol for protein kinase C activation, Biochem. Biophys. Res. Commun. 144 (2) (1987) 598–605.
[16] P.A. Marignani, R.M. Epand, R.J. Sebaldt, Acyl chain dependence of diacylglycerol activation of protein kinase C activity in vitro, Biochem. Biophys. Res. Commun. 225 (2) (1996) 469–473.
[17] Y. Kamiya, S. Mizuno, S. Komenoi, H. Sakai, F. Sakane, Activation of conventional and novel protein kinase C isozymes by different diacylglycerol molecular species, Biochem. Biophys. Rep. 7 (2016) 361–366.
[18] D. Armstrong, R. Zidovetzki, Amplification of diacylglycerol activation of protein kinase C by cholesterol, Biophys. J. 94 (12) (2008) 4700–4710.
[19] R.M. Epand, Lipid polymorphism and protein–lipid interactions, Biochim. Biophys. Acta (BBA) - Rev. Biomembr. 1376 (3) (1998) 353–368.
[20] J.C. Gómez-Fernández, S. Corbalán-García, Diacylglycerols, multivalent membrane modulators, Chem. Phys. Lipids 148 (1) (2007) 1–25.
[21] M. Alwarawrah, J. Dai, J. Huang, Modification of lipid bilayer structure by diacylglycerol: A comparative study of diacylglycerol and cholesterol, J. Chem. Theory Comput. 8 (2) (2012) 749–758.
[22] L. Vamparys, R. Gautier, S. Vanni, W.D. Bennett, D.P. Tieleman, B. Antonny, C. Etchebest, P.F. Fuchs, Conical lipids in flat bilayers induce packing defects similar to that induced by positive curvature, Biophys. J. 104 (3) (2013) 585–593.

[23] M. Alwarawrah, F. Hussain, J. Huang, Alteration of lipid membrane structure and dynamics by diacylglycerols with unsaturated chains, Biochim. Biophys. Acta (BBA) - Biomembr. 1858 (2) (2016) 253–263.

[24] H. Saito, T. Morishita, T. Mizukami, K.I. Nishiyama, K. Kawaguchi, H. Nagao, Molecular dynamics study of binary POPC bilayers: Molecular condensing effects on membrane structure and dynamics, 1136 (2018). Export Date: 22 February 2019.

[25] P. Campomanes, V. Zoni, S. Vanni, Local accumulation of diacylglycerol alters membrane properties nonlinearly due to its transbilayer activity, Commun. Chem. 2 (1) (2019).

[26] G. Enkavi, M. Javanainen, W. Kulig, T. Róg, I. Vattulainen, Multiscale simulations of biological membranes: The challenge to understand biological phenomena in a living substance, Chem. Rev. 119 (9) (2019) 5607–5774.

[27] A. Magarkar, P. Parkkila, T. Viitala, T. Lajunen, E. Mobarak, G. Licari, O. Cramariuc, E. Vauthey, T. Róg, A. Bunker, Membrane bound COMT isoform is an interfacial enzyme: general mechanism and new drug design paradigm, Chem. Commun. 54 (2018) 3440–3443.

[28] S. Lautala, R. Provenzani, A. Koivuniemi, W. Kulig, V. Talman, T. Róg, R.K. Tuominen, J. Yli-Kauhaluoma, A. Bunker, Rigorous computational study reveals what docking overlooks: Double trouble from membrane association in protein kinase C modulators, J. Chem. Inf. Model. 60 (11) (2020) 5624–5633, PMID: 32915560.

[29] W.F.D. Bennett, D.P. Tieleman, Molecular simulation of rapid translocation of cholesterol, diacylglycerol, and ceramide in model raft and nonraft membranes, J. Lipid Res. 53 (3) (2012) 421–429.

[30] F. Ogushi, R. Ishitsuka, T. Kobayashi, Y. Sugita, Rapid flip-flop motions of diacylglycerol and ceramide in phospholipid bilayers, Chem. Phys. Lett. 522 (2012) 96–102.

[31] J.A. Hamilton, S.P. Bhamidipati, D.R. Kodali, D.M. Small, The interfacial conformation and transbilayer movement of diacylglycerols in phospholipid bilayers, J. Biol. Chem. 266 (2) (1991) 1177–1186.

[32] K. Schorn, D. Marsh, Lipid chain dynamics and molecular location of diacylglycerol in hydrated binary mixtures with phosphatidylcholine: Spin label ESR studies, Biochemistry 35 (12) (1996) 3831–3836.

[33] A. Zachowski, Phospholipids in animal eukaryotic membranes: Transverse asymmetry and movement, Biochem. J. 294 (1) (1993) 1–14.

[34] M. Ikeda, A. Kihara, Y. Igarashi, Lipid asymmetry of the eukaryotic plasma membrane: Functions and related enzymes, Biol. Pharm. Bull. 29 (8) (2006) 1542–1546.

[35] A. Chakrabarti, Phospholipid asymmetry in biological membranes: Is the role of phosphatidylethanolamine underappreciated? J. Membr. Biol. 254 (2) (2021) 127–132.

[36] A. Naudí, R. Cabré, M. Jové, V. Ayala, H. Gonzalo, M. Portero-Otín, I. Ferrer, R. Pamplona, Lipidomics of Human Brain Aging and Alzheimer's Disease Pathology, in: International Review of Neurobiology, vol. 122, 2015.

[37] T. Harayama, H. Riezman, Understanding the diversity of membrane lipid composition, Nat. Rev. Mol. Cell Biol. 19 (5) (2018) 281–296.

[38] T. Róg, M. Pasenkiewicz-Gierula, I. Vattulainen, M. Karttunen, Ordering effects of cholesterol and its analogues, Biochim. Biophys. Acta (BBA) - Biomembr. 1788 (1) (2009) 97–121, Lipid Interactions, Domain Formation, and Lateral Structure of Membranes.

[39] B.R. Brooks, C.L. Brooks III, A.D. Mackerell Jr., L. Nilsson, R.J. Petrella, B. Roux, Y. Won, G. Archontis, C. Bartels, S. Boresch, A. Caflisch, L. Caves, Q. Cui, A.R. Dinner, M. Feig, S. Fischer, J. Gao, M. Hodoscek, W. Im, K. Kuczera, T. Lazaridis, J. Ma, V. Ovchinnikov, E. Paci, R.W. Pastor, C.B. Post, J.Z. Pu, M. Schaefer, B. Tidor, R.M. Venable, H.L. Woodcock, X. Wu, W. Yang, D.M. York, M. Karplus, CHARMM: The biomolecular simulation program, J. Comput. Chem. 30 (10) (2009) 1545–1614.

[40] S. Jo, T. Kim, V.G. Iyer, W. Im, CHARMM-GUI: A web-based graphical user interface for CHARMM, J. Comput. Chem. 29 (11) (2008) 1859–1865.

[41] J. Lee, X. Cheng, J.M. Swails, M.S. Yeom, P.K. Eastman, J.A. Lemkul, S. Wei, J. Buckner, J.C. Jeong, Y. Qi, S. Jo, V.S. Pande, D.A. Case, C.L. Brooks III, A.D. MacKerell Jr., J.B. Klauda, W. Im, CHARMM-GUI input generator for NAMD, GROMACS, AMBER, OpenMM, and CHARMM/OpenMM simulations using the CHARMM36 additive force field, J. Chem. Theory Comput. 12 (1) (2016) 405–413.

[42] I. Gould, A. Skjevik, C. Dickson, B. Madej, R. Walker, Lipid17: A comprehensive AMBER force field for the simulation of zwitterionic and anionic lipids, 2018, Manuscript in Preparation.

[43] C.J. Dickson, B.D. Madej, A.A. Skjevik, R.M. Betz, K. Teigen, I.R. Gould, R.C. Walker, Lipid14: The amber lipid force field, J. Chem. Theory Comput. 10 (2) (2014) 865–879.

[44] W.L. Jorgensen, J. Chandrasekhar, J.D. Madura, R.W. Impey, M.L. Klein, Comparison of simple potential functions for simulating liquid water, J. Chem. Phys. 79 (2) (1983) 926–935.

[45] C.I. Bayly, P. Cieplak, W.D. Cornell, P.A. Kollman, A well-behaved electrostatic potential based method using charge restraints for deriving atomic charges: The RESP model, J. Phys. Chem. 97 (40) (1993) 10269–10280.

[46] A.A. Skjevik, B.D. Madej, R.C. Walker, K. Teigen, LIPID11: A modular framework for lipid simulations using amber, J. Phys. Chem. B 116 (36) (2012) 11124–11136.

[47] H.J.C. Berendsen, D. van der Spoel, R. van Drunen, GROMACS: A message-passing parallel molecular dynamics implementation, Comput. Phys. Comm. 91 (1–3) (1995) 43–56.

[48] D.V.D. Spoel, E. Lindahl, B. Hess, G. Groenhof, A.E. Mark, H.J.C. Berendsen, GROMACS: Fast, flexible, and free, J. Comput. Chem. 26 (16) (2005) 1701–1718.

[49] M.J. Abraham, T. Murtola, R. Schulz, S. Páll, J.C. Smith, B. Hess, E. Lindah, Gromacs: High performance molecular simulations through multi-level parallelism from laptops to supercomputers, SoftwareX 1–2 (2015) 19–25.

[50] M. Abraham, D. van der Spoel, E. Lindahl, B. Hess, GROMACS the development team, GROMACS user manual version 2018.6, 2019.

[51] The GROMACS development team, GROMACS documentation release 2021.2, 2021.

[52] W.F.V. Gunsteren, H.J.C. Berendsen, A leap-frog algorithm for stochastic dynamics, Mol. Simul. 1 (3) (1988) 173–185.

[53] U. Essmann, L. Perera, M.L. Berkowitz, T. Darden, H. Lee, L.G. Pedersen, A smooth particle mesh Ewald method, J. Chem. Phys. 103 (19) (1995) 8577–8593.

[54] B. Hess, H. Bekker, H.J.C. Berendsen, J.G.E.M. Fraaije, LINCS: A linear constraint solver for molecular simulations, J. Comput. Chem. 18 (12) (1997) 1463–1472.

[55] S. Nosé, A molecular dynamics method for simulations in the canonical ensemble, Mol. Phys. 52 (2) (1984) 255–268.

[56] W.G. Hoover, Canonical dynamics: Equilibrium phase-space distributions, Phys. Rev. A 31 (3) (1985) 1695–1697.

[57] M. Parrinello, A. Rahman, Polymorphic transitions in single crystals: A new molecular dynamics method, J. Appl. Phys. 52 (12) (1981) 7182–7190.

[58] M.J. Abraham, D. van der Spoel, E. Lindahl, B. Hess, GROMACS the development team, GROMACS user manual version 2018.7, 2019.

[59] S. Kumar, J.M. Rosenberg, D. Bouzida, R.H. Swendsen, P.A. Kollman, The weighted histogram analysis method for free-energy calculations on biomolecules. I. The method, J. Comput. Chem. 13 (8) (1992) 1011–1021.

[60] J.S. Hub, B.L.D. Groot, D.V.D. Spoel, G-whams-a free weighted histogram analysis implementation including robust error and autocorrelation estimates, J. Chem. Theory Comput. 6 (12) (2010) 3713–3720.

[61] S.M. Yee, R.J. Gillams, S.E. McLain, C.D. Lorenz, Effects of lipid heterogeneity on model human brain lipid membranes, Soft Matter 17 (2021) 126–135.

[62] J. Huang, G.W. Feigenson, A microscopic interaction model of maximum solubility of cholesterol in lipid bilayers, Biophys. J. 76 (4) (1999) 2142–2157.

[63] G. Zhang, M.G. Kazanietz, P.M. Blumberg, J.H. Hurley, Crystal structure of the Cys2 activator-binding domain of protein kinase Cδ in complex with phorbol ester, Cell 81 (6) (1995) 917–924.

[64] J. Li, B.P. Ziemba, J.J. Falke, G.A. Voth, Interactions of protein kinase C-α C1A and C1B domains with membranes: A combined computational and experimental study, J. Am. Chem. Soc. 136 (33) (2014) 11757–11766.

[65] J.R. Giorgione, J.-H. Lin, J. McCammon, A.C. Newton, Increased membrane affinity of the C1 domain of protein kinase cδ compensates for the lack of involvement of its C2 domain in membrane recruitment, J. Biol. Chem. 281 (3) (2006) 1660–1669.

[66] D.R. Dries, L.L. Gallegos, A.C. Newton, A single residue in the C1 domain sensitizes novel protein kinase C isoforms to cellular diacylglycerol production, J. Biol. Chem. 282 (2) (2007) 826–830.

[67] S. Madani, A. Hichami, A. Legrand, J. Belleville, N.A. Khan, Implication of acyl chain of diacylglycerols in activation of different isoforms of protein kinase C, FASEB J. 15 (14) (2001) 2595–2601.

[68] S.M. Ryckbosch, P.A. Wender, V.S. Pande, Molecular dynamics simulations reveal ligand-controlled positioning of a peripheral protein complex in membranes, Nature Commun. 8 (1) (2017) 6.

[69] H. Yang, D. Staveness, S.M. Ryckbosch, A.D. Axtman, B.A. Loy, A.B. Barnes, V.S. Pande, J. Schaefer, P.A. Wender, L. Cegelski, REDOR NMR reveals multiple conformers for a protein kinase C ligand in a membrane environment, ACS Cent. Sci. 4 (1) (2018) 89–96.

[70] D.P. Tieleman, J.L. MacCallum, W.L. Ash, C. Kandt, Z. Xu, L. Monticelli, Membrane protein simulations with a united-atom lipid and all-atom protein model: Lipid-protein interactions, side chain transfer free energies and model proteins, J. Phys. Condens. Matter 18 (28) (2006).

[71] H.S. Antila, B. Kav, M.S. Miettinen, H. Martinez-Seara, P. Jungwirth, O.H.S. Ollila, Emerging era of biomolecular membrane simulations: Automated physically-justified force field development and quality-evaluated databanks, 2022, http://dx.doi.org/10.26434/chemrxiv-2022-x4z6k, ChemRxiv, This content is a preprint and has not been peer-reviewed.

[72] H.S. Antila, A. Wurl, O.H. Ollila, M.S. Miettinen, T.M. Ferreira, Rotational decoupling between the hydrophilic and hydrophobic regions in lipid membranes, Biophys. J. 121 (1) (2022) 68–78.

[73] F. Leeb, L. Maibaum, Spatially resolving the condensing effect of cholesterol in lipid bilayers, Biophys. J. 115 (11) (2018) 2179–2188.

[74] T. Kano-Sueoka, M.E. Nicks, Abnormal function of protein kinase c in cells having phosphatidylethanolamine-deficient and phosphatidylcholine-excess membranes, Cell Growth Differ.: Mol. Biol. J. Am. Assoc. Cancer Res. (ISSN: 10449523) 4 (7) (1993) 533–537.

[75] M.D. Bazzi, M.A. Youakim, G.L. Nelsestuen, Importance of phosphatidylethanolamine for association of protein kinase C and other cytoplasmic proteins with membranes, Biochemistry 31 (1992) 1125–1134.

[76] G. Senisterra, R.M. Epand, Role of membrane defects in the regulation of the activity of protein kinase C, Arch. Biochem. Biophys. 300 (1) (1993) 378–383.
[77] S.J. Slater, M.B. Kelly, F.J. Taddeo, C. Ho, E. Rubin, C.D. Stubbs, The modulation of protein kinase C activity by membrane lipid bilayer structure, J. Biol. Chem. 269 (7) (1994) 4866–4871.
[78] S.R. Shaikh, M.R. Brzustowicz, W. Stillwell, S.R. Wassall, Formation of inverted hexagonal phase in SDPE as observed by solid-state 31P NMR, Biochem. Biophys. Res. Commun. 286 (4) (2001) 758–763.
[79] X. Wang, P.J. Quinn, Cubic phase is induced by cholesterol in the dispersion of 1-palmitoyl-2-oleoyl-phosphatidylethanolamine, Biochim. Biophys. Acta (BBA) - Biomembr. 1564 (1) (2002) 66–72.
[80] R.M. Epand, R. Bottega, Modulation of the phase transition behavior of phosphatidylethanolamine by cholesterol and oxysterols, Biochemistry 26 (7) (1987) 1820–1825.
[81] R.M. Epand, Diacylglycerols, lysolecithin, or hydrocarbons markedly alter the bilayer to hexagonal phase transition temperature of phosphatidylethanolamines, Biochemistry 24 (25) (1985) 7092–7095.
[82] F.M. Goñi, The basic structure and dynamics of cell membranes: An update of the Singer–Nicolson model, Biochim. Biophys. Acta (BBA) - Biomembr. 1838 (6) (2014) 1467–1476.
[83] H.T. McMahon, E. Boucrot, Membrane curvature at a glance, J. Cell Sci. 128 (6) (2015) 1065–1070.
[84] A.E. Drobnies, S.M. Davies, R. Kraayenhof, R.F. Epand, R.M. Epand, R.B. Cornell, CTP:phosphocholine cytidylyltransferase and protein kinase c recognize different physical features of membranes: differential responses to an oxidized phosphatidylcholine, Biochim. Biophys. Acta (BBA) - Biomembr. 1564 (1) (2002) 82–90.
[85] Y.A. Hannun, C.R. Loomis, R.M. Bell, Activation of protein kinase C by Triton X-100 mixed micelles containing diacylglycerol and phosphatidylserine, J. Biol. Chem. 260 (18) (1985) 10039–10043.
[86] R. Epand, N. Fuller, R. Rand, Role of the position of unsaturation on the phase behavior and intrinsic curvature of phosphatidylethanolamines, Biophys. J. 71 (4) (1996) 1806–1810.
[87] J.R. Giorgione, Z. Huang, R.M. Epand, Increased activation of protein kinase C with cubic phase lipid compared with liposomes, Biochemistry 37 (8) (1998) 2384–2392, PMID: 9485386.
[88] J.C. Bozelli, R.M. Epand, Membrane shape and the regulation of biological processes, J. Mol. Biol. 432 (18) (2020) 5124–5136.